https://doi.org/10.26682/ajuod.2023.26.2.13
Journal of University of Duhok., Vol. 26, No.2 (Agri. and Vet. Sciences), Pp 127-143, 2023

TREND ANALYSIS, MODELING AND INTERPOLATION OF REFERENCE EVAPOTRANSPIRATION TIME SERIES IN THE SEMI ARID REGION OF DUHOK GOVERNORATE

MARWAN **B**ASHEER **I**SMAIL **G**OVAY[*] and **T**ARIQ **H**AMA **K**ARIM[**]
[*]Dept. of Soil and Water., College of Agricultural Engineering Sciences, University of Duhok, Kurdistan Region-Iraq
[**]Dept. of Survey and Geomatics Engineering, Faculty of Engineering, Tishk International University, Erbil, Kurdistan Region-Iraq

(Received: November 7, 2023; Accepted for Publication: December 24, 2023)

ABSTRACT

Reference Evapotranspiration (ET_o) is one of the most important components of the hydrologic cycle. Its assessment, forecasting, spatial interpolation besides climate change effects on this variable are supportive in applying management techniques to water resources and in determining appropriate adaptation strategies. Hence, this study was initiated to forecast, detect changes and generate surface maps for ET_o time series at different time scales. The datasets for this investigation encompassed the input climatic parameters from 12 stations within Duhok governorate for a time span varied from 18 to 20 years for estimating reference evapotranspiration according to penman-Monteith formula. The results indicated that about 17% of stations exhibited increasing trend in annual ET, while the remaining station exhibited significant and non-significant decreasing trends. Spearman rank test Sen's slope and linear regression analysis offered slopes of similar signs but of different magnitudes. Seasonal ARIMA model denoted as (1, 1, 1)(0, 1, 1)$_{12}$ was the most appropriate model for predicting monthly ET_o time series at more than 90% of study stations. The indicated model predicted the monthly ET_o with a reasonable accuracy for the coming 36 months. Further, the results indicated that in general, the IDW and spline schemes method exhibited highest and lowest accuracy in most cases. Judging from several performance indicators, it can be inferred IDW, OK and UK methods yielded comparable results.

KEYWORDS: Reference evapotranspiration, forecasting, trend analysis, interpolation methods

1. INTRODUCTION

Reference evapotranspiration is a key parameter for many agricultural issues and hydrologic processes as crop water requirement, irrigation schedule, water resource management, etc. (Mardikis et al., 2004). Marino et al. (1993) also revealed that determination of evapotranspiration can be considered as the first step for specifying irrigation water requirements for use in design and operation of water projects.

Time series analysis has quickly developed from both theoretical and practical aspects during the last few decades for forecasting and management. It has many applications in modern water resources management, such as water supply planning, water quality management, irrigation system, hydropower generation, and sustainable utilization of water resources etc (Wang et al., 2009; Zhang et al., 2011). The type of data used for analysis should be generally related to data which are autocorrelated (Asadi et al., 2013). There are a host of techniques for forecasting evapotranspiration. Example of such models are autoregressive (AR), moving average (MA), autoregressive moving average (ARMA), autoregressive integrated moving average (ARIMA), Thomas Feiring, etc (Gautam, and Sinha, 2016). It was observed that within the aforementioned models ARIMA model has been found to be more appropriate for analysis and forecasting of hydrological events.

Time series modeling has been used for forecasting evapotranspiration under different climatic conditions and at different time scales. For instance, Gautam and Sinha (2016) used SARIMA in Bokaro district, India for forecasting monthly evapotranspiration with a reasonable level of accuracy; Alhassounl et al. (1997) built autoregressive models for ten different stations at Saudi Arabia; Valipour

(2012) developed ARIMA model for Mehrabad station, Iran; Mohan and Arumugam (1995) analyzed ARIMA modelling of weekly data of evapotranspiration at Annamlainagar station, India.

Shenbin et al. (2006) reported that recently the focus is on temperature and precipitation variability to monitor climatic change. Apart from the fact that the evapotranspiration is the third important climatic factor, it has received a lesser amount of attention. The greater importance of evapotranspiration more than the two-abovementioned parameters lies in the fact that it controls mass and energy exchange between the atmosphere and terrestrial ecosystem.

Goroshi et al. (2017) elucidated that studies on evapotranspiration have exhibited both decreasing and increasing trend in different regions of the world since the mid of the twenty century. Tabari et al. (2013) analyzed the PMF-56 potential evapotranspiration at different time scales recorded at 20 meteorological stations from 1966 to 2005 in the western part of Iran using the Mann-Kendall test and their results indicated that the annual potential evaporation has a positive trend in most of the study stations. Similarly, it was observed that winter potential evapotranspiration time series exhibited an increasing trend in the Kashmir valley over the period from 1901 to 2002 at a 95% confidence level. In contrast, in another study by Xu et al. (2006), it was noticed that the annual evapotranspiration was characterized by having a decreasing trend. They attributed the downward trend chiefly to a considerable decrease in the net total radiation and to a lesser extent to a significant drop in the wind speed over the Changjiang catchment, China over the time span from 1960 to 2000.

As a result of the lack of consistent spatial time series data on evapotranspiration, limited studies have been carried out on potential evapotranspiration trend in the region under study and over the country as a whole.

To date, a host of interpolation techniques have been used for interpolating climatic variables, ranging from simple techniques such as IDW, thin plate splines to more sophisticated geostatistical methods such as kriging and its variants.

The results from different spatial interpolation methods unveiled substantial differences among the interpolation techniques. The differences among different methods stem from the nature of climatic parameter, the drawn assumptions and data's spatial configuration, etc. (Nalder and Wein, 1998).

Hodum et al. (2017) studied the spatial distribution of potential evapotranspiration based on the means of 32 years for monthly data recorded at 131 Indian meteorological stations. They revealed that IDW outperformed kriging method in almost all the cases, thus it was recommended for interpolation of potential evapotranspiration and its input meteorological parameters. Gong et al. (2005) reported that among commonly used interpolation methods, Ordinary Kriging offered the best performance. From the interpolation results, regional maps of seasonal and annual reference evapotranspiration were generated in a GIS environment. These regional maps provide a reasonable way to fill in the gaps between discrete spatial data.

It has been shown that Penman-Monteith equation outperforms other techniques under varying conditions (Allen et al., 1998). This method is requiring data collection on several climatic parameters that are unavailable at most of the locations within the study area. An alternative approach consists in using spatial interpolation to estimate the value of missing variables at the desired locations. (Tomas-Burguera., 2017). Hence, the current study was proposed to analyze the reference evapotranspiration time series at the Duhok governorate via targeting the following specific objectives:

1) To establish a time series model to analyze and forecast reference evapotranspiration for the existing meteorological stations within the study area.
2) To investigates the historical trend of reference evapotranspiration over the study area.
3) To detect abrupt changes in reference evapotranspiration over the study area during the period of record.
4) To generate a map of the Duhok province for evapotranspiration at different scales.

2. MATERIALS AND METHODS

2.1. Data Acquisition

The collected datasets encompassed the input climatic parameters required for estimating reference evapotranspiration according to Penman-Monteith. They were recorded at 12 meteorological stations distributed over the study area (Fig. 1) for a period from 1998 to 2020. The recorded parameters were monthly average daily maximum temperature (Tmax), monthly average daily minimum temperature

(Tmin), Actual vapor pressure (ea), monthly average daily wind speed (u_2) at a height of 2m above the ground, monthly average sunshine duration (n), and geographical coordinates of each station along with their altitudes.

Most of the database was provided from the Ministry of agriculture and Water Resources, the Directorate of Duhok meteorology and the General Directorate of meteorology and Seismology.

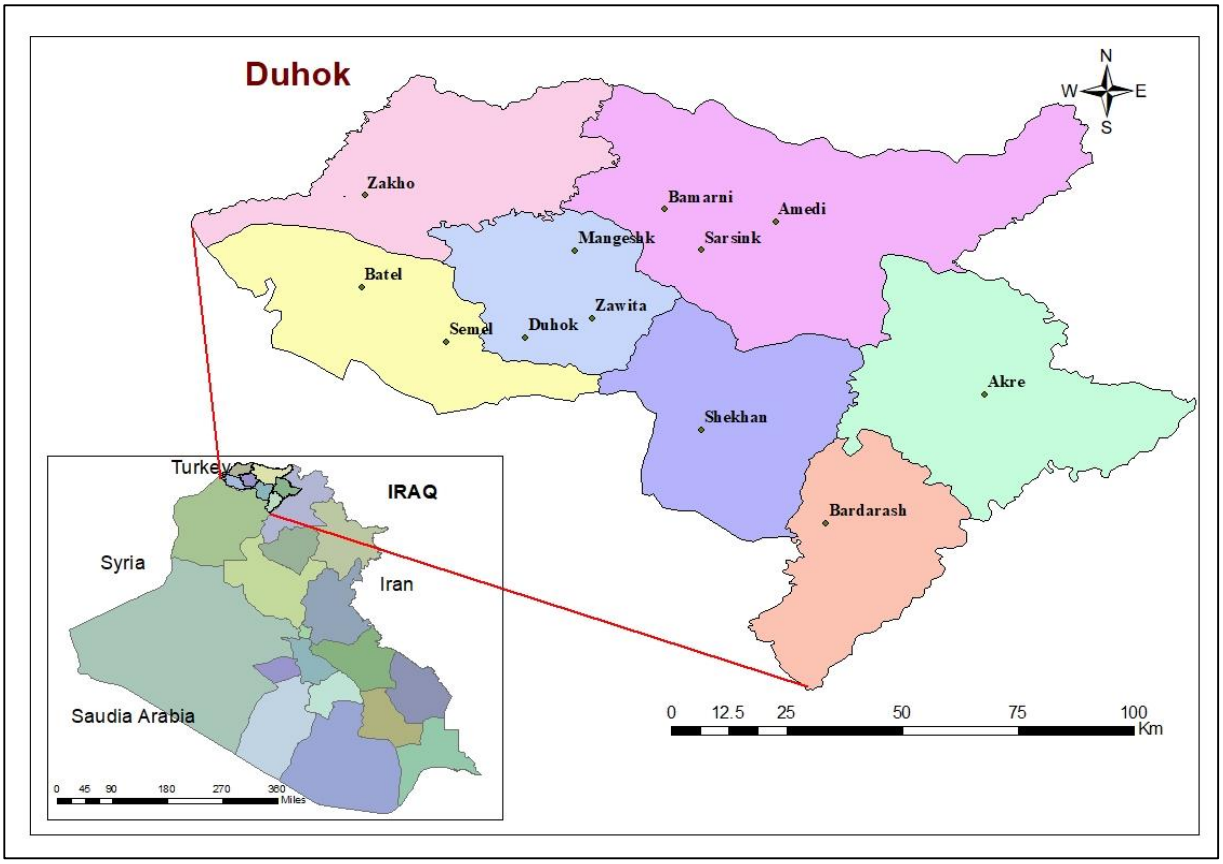

Fig (1): Location map showing the distribution of meteorological stations over the study area.

2.2. Estimation of reference evapotranspiration

The reference evapotranspiration (ETo) in mm day^{-1} was estimated according to the formula proposed by Penman-Monteith (Allen et al., 1998):

$$ET_o = \frac{0.408\Delta(R_n - G)}{\Delta + \gamma(1 + 0.34U_2)} + \frac{\gamma U_2 (e_s - e_a)\frac{900}{T+273}}{\Delta + \gamma(1 + 0.34U_2)}$$

.....1

where Δ: slope of vapor pressure versus temperature curve [kPa °C^{-1}], Rn: net radiation [MJ m^{-2} day^{-1}], G: heat flux density into and out of the soil [MJ m^{-2} day^{-1}], T: mean daily air temperature at a height of 2 m [°C], U2: wind speed at a height of 2 m [m s^{-1}], e_s: saturation vapor pressure [kPa], e_a: actual vapor pressure [kPa], γ: psychrometric constant [kPa °C^{-1}]. It is commendable to mention that the CROPWAT software version8 was used for generation the ET_o time series.

Prior to the data analysis, four homogeneity tests were conducted, namely, standard normal homogeneity test (SNHT), Buishand range (BR) test, Pettitt test (PT), and Von Neumann ratio (VNR) to show whether the computed reference evapotranspiration time series at different time scales were affected by non-climatic factors using IBM-SPSS V23.

Before fitting an ARIMA model, the data were examined for stationarity. Augmented Dickey-Fuller Unit Root test was also employed to verify non-stationarity of the data using EViews10 software. Differences of lag K=1 and 12 were taken to remove seasonality and nonstationarity for monthly and annual evapotranspiration data respectively. The Box-Jenkins methodology was followed to built the ARIMA model. Autocorrelation and partial

Autocorrelation charts were used to identify the order of each of the autoregressive and moving average models. These functions were also used to check detrending and Deseasonality after differencing.

During the next step, the parameters of tentatively identified model were estimated using non-linear optimization technique.

At the last stage of model, building diagnostic checking was made to show whether the residuals are normally distributed, homoscedastic and independent. Ljung-Box test was also performed to examine the goodness of the trial models:

$$Q = n(n+2)\sum_{k=1}^{m}\frac{r^2_k}{n-k} \quad \ldots\ldots\ldots\ldots\ldots\ldots 2$$

Where n= the sample size, k = autocorrelation at lag k and m is the number of lagged to be examined. When the model failed to meet the requirement, the model was dropped, were correlated, then the model was dropped and new trials were made until an appropriate model was achieved. To prevent overfitting fitting errors, AIC and EF criterion was employed.

Further, the performance of the forecasting models was assessed and compared by using standard metrics such as MAE, and MAPE, RMSE and CRM and D.

2. 3. Trend Analysis

Parametric (regression analysis) and non-parametric (Mann-Kendall) tests were employed to detect trends in the historical reference potential evapotranspiration data. The later test is distribution free and unaffected by outliers. Further, the cumulative sum (CUMUM) was used to detect abrupt changes or sequential shift in evapotranspiration time series. Additionally, Sen's slope method was used to compute magnitude of trend line.

2.4 . Reference Evapotranspiration Forecasting

Upon specifying the best model from the historical data, forecasting was done for the next incoming five years using IBM SPSS version 23.

2.5. Interpolation Schemes.

To transform the discrete values into a continuous spatial pattern over Duhok Governorate, different algorithms (conventional and geostatistical approaches) with default input parameters (Mitas and Mitasova,1999) were employed using ESRI ArcMap Ver.10.8. The interpolation methods encompassed; IDW, Ordinary Kriging, Universal Kriging and spline. The suitability of the prediction methods was examined via leave-one-out cross-validation ((LOOCV) (Chilès and Delfner 2012). A host of performance criteria (MAE, MAPE, MRSE, D and NSE) was also used for selecting the most appropriate interpolation method. The Technique for Order Preference by Similarity to Ideal Solution or TOPSIS technique was also employed for ranking the interpolation techniques (Govay and Karim, 2023).

3. RESULTS AND DISCUSSION

3.1. Descriptive statistics

Table1 portrays the summary of descriptive statistics for 12 stations distributed over the study area. The aggregated data is composed of annual reference evapotranspiration time series that was based on monthly data computed over the last two decades. As can be seen, the mean annual reference evapotranspiration varies from as low as 1195.19 mm for Sarsing station to as high as 1459.03 mm for Shekhan station and the values for the remaining stations fall between these two extremes.

It is also obvious from Table1 that the coefficient of temporal variability over the study period ranged from a minimum of 3.92% for Zakho station to a maximum of 9.10% for Mangeshk station. Based on the classification scheme proposed by Gomes (1985), only Akre, Semel and Mangeshk fell in the medium class c (20% < CV <10%), while the remaining stations fell in the low class (CV %< 10%). On the other hand, it was observed that the evapotranspiration varied spatially by 8.22%.

Additionally, the results also indicted that the reference evapotranspiration at 3 stations out of 12% were positively skewed, i.e., it is skewed to the right. On the other hand, this parameter was negatively skewed at the remaining stations. Further, it can be noticed that with one exception, the skewness lies between -1 and +1, indicating that the employed data did not deviated considerably from normal distribution. Virgilio et al., 2007; PazGonzales et al., 2000 elucidated that when the skewness of a given data lies between -1 and +1, it can be considered as normally distributed data.

It is commendable to mention that the skewness was very close to 0 at some stations such as Zakho, Bardarash and Batel, indicating that distribution was very close to perfect normal distribution.

Table (1): Descriptive statistics of stations annual ET_0 data series**.**

Stations	N	Minimum	Maximum	Mean	Std. Deviation	CV%	Skewness		Kurtosis	
							Statistic	Std. Error	Statistic	Std. Error
Duhok	21	1124.80	1455.82	1335.72	88.88	4.46	-0.681	0.501	0.146	0.972
Zakho	20	1189.46	1355.23	1297.29	50.85	6.97	-0.973	0.512	0.043	0.992
Akre	20	1314.09	1573.34	1415.92	63.18	4.58	0.787	0.512	0.681	0.992
Amedi	20	1140.56	1493.99	1288.62	89.87	4.78	0.609	0.512	0.150	0.992
Semel	20	1157.52	1545.72	1367.42	95.03	4.08	-0.258	0.512	-0.071	0.992
Zawita	20	1078.62	1395.86	1279.47	69.78	6.65	-1.386	0.512	3.090	0.992
Shekhan	20	1320.85	1585.62	1459.03	62.11	9.1	-0.118	0.512	0.402	0.992
Sarsing	20	1060.18	1280.58	1195.19	59.72	5	-0.984	0.512	0.574	0.992
Bardarash	20	1330.69	1545.82	1446.73	69.21	6.95	-0.066	0.512	-1.159	0.992
Mangeshk	18	994.40	1461.41	1322.27	120.31	4.26	-1.513	0.536	2.031	1.038
Bamarne	18	1209.56	1485.89	1400.94	64.11	3.92	-1.470	0.536	3.738	1.038
Batel	18	1313.95	1483.03	1400.40	57.18	5.45	0.086	0.536	-1.330	1.038

It is also evident from Table 1 that with two exception that kurtosis value is less than 3. a kurtosis value less than three implies a negative kurtosis or platykurtic. The platykurtic distribution is heavy-tailed, and the peak can be flatter (Menon, 2023).

The box-whisker plot displayed in Fig. 2 revealed that the median line of the box did shift away from the center of box in most of the stations. This is an additional confirmation for the slight deviation of the reference evapotranspiration data from normal distribution. It can also be elucidated that the dataset for most of that stations is free of outliers. On the other hand, those of the remaining stations have a few outliers.

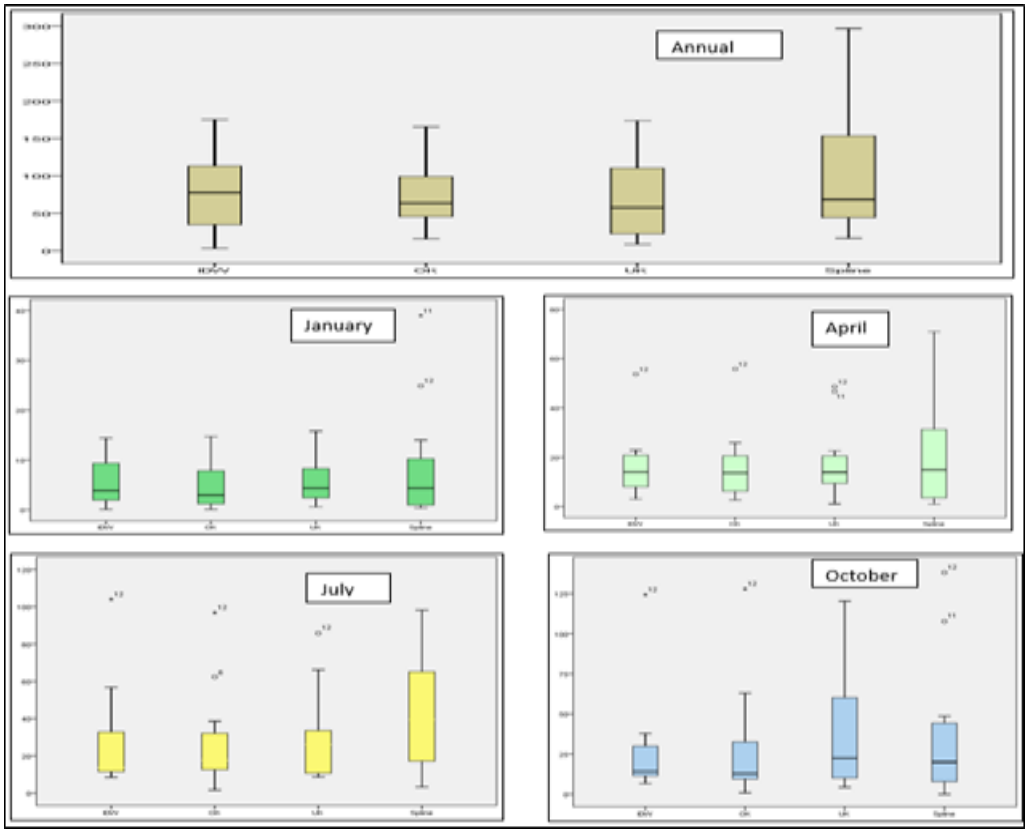

Fig (2): Description of the Error of estimation by different interpolation methods by Box and whisker plots for residual of annual ET_0 and monthly ET_0.

3.2. Homogeneity Test

Four commonly used statistical tests were used to the annual time series to test for their homogeneity (Table 2). The tests encompassed Pettitt, SNHT, Buishand and VNR. All of these tests assumed the null hypothesis of dataset being homogeneous. The results indicated that the stations with time span of less than 17 years fell in the suspect class. These stations were Bardarash, Mangeshk, Bamarni and Batel. The inhomogeneity in climatic data can be accredited to many factors, like human mishandling, instrumentation error and changes in the environmental changes nearby the instrument (Capozzi et al., 2020). Accordingly, it is recommended not to use these data for further analysis before correction or before expanding the database (Wijngaard et al., 2003). Agha et al. (2017) reported that the correction of inhomogeneous time series is a crucial step before its use in trend analysis.

Table (2): Results of homogeneity tests for the annual evapotranspiration recorded at the study stations.

#	Stations	Pettit's test		SNHT test		Buishand test		VON test		Class	Results
		K or kn	P-value	T0	P-value	Q	P-value	N	P-value		
1	Duhok	48	0.585	2.828	0.614	3.656	0.397	1.574	0.162	Class A	Useful
2	Zakho	77	0.015	12.1	0.003	6.911	0.003	0.769	0.002	Class C	Suspect
3	Akre	54	0.257	5.049	0.223	4.29	0.208	1.71	0.258	Class A	Useful
4	Amedi	76	0.016	10.754	0.002	6.662	0.004	0.841	0.002	Class C	Suspect
5	Semel	56	0.221	6.915	0.043	4.925	0.099	1.142	0.017	Class B	Doubtful
6	Zawita	47	0.489	3.815	0.337	3.084	0.539	1.841	0.332	Class A	Useful
7	Shekhan	49	0.428	5.264	0.144	4.667	0.124	1.788	0.313	Class A	Useful
8	Sarsing	68	0.051	4.939	0.225	4.961	0.089	1.050	0.013	Class A	Useful
9	Bardarash	92	0.000	12.496	0.000	7.946	0.000	0.712	0.001	Class C	Suspect
10	Mangeshk	56	0.069	13.162	0.000	6.585	0.001	0.739	0.003	Class C	Suspect
11	Bamarni	46	0.267	3.269	0.418	2.481	0.778	2.256	0.714	Class A	Useful
12	Batel	37	0.649	3.821	0.305	3.180	0.463	1.735	0.281	Class A	Useful

3.3 .Trend Analysis

Table 3 exhibits parametric (linear regression) and non-parametric methods (Mann-Kendall, slope and Spearman rank test) for trend identification of annual reference evapotranspiration at the existing stations over the study area. As can be noticed in Table 3 that the evapotranspiration had a mixture of increasing, decreasing trends and no trend. Out of 12 stations only two stations, namely, Amedi and Bamarne exhibited increasing trends based on Mann-Kendall test. Bamarni offered the highest increasing (positive) ET_0 trend of 1.97 mm yr^{-1}, followed by Amedi with an increasing trend of 7.81 mm yr^{-1}. In contrast, four stations: Zakho, Sarsing, Bardarash and Mangeshk showed decreasing trends. Mangeshk station exhibited the maximum decreasing trend of 15.87 mm yr^{-1}, while Sarsing showed a minimum decreasing trend of 4.29 mm yr^{-1}. Unlike these stations, Duhok, Semel, Zawita and Shekhan exhibited no significant trend.

Table (3): Trend analysis of annual ET_0 time series recorded at some selected meteorological stations over the study area.

#	Station	Mann-Kendall and Sen's slope tests				Spearman's rho Test Statistic, ZSP	Slope of regression line	R^2
		Z-Statistic	P	Sen's slope	Trend			
1	**Duhok**	-1.7	0.880	-0.556	NT	-0.070	-0.162	0.0001
2	**Zakho**	-2.6	0.006	-5.807	DT	-2.070	-5.781	0.443
3	**Akre**	1.72	0.086	4.164	NT	1.334	4.621	0.187
4	**Amedi**	2.08	0.025	8.206	IT	1.526	7. 811	0.264
5	**Semel**	-1.4	0.173	-6.784	NT	1.606	-4.962	0.095
6	**Zawita**	-1.2	0.230	-1.758	NT	-0.998	-0.757	0.004
7	**Shekhan**	-1.07	0.284	-3.296	NT	-0.694	-3.436	0.107
8	**Sarsing**	-2.27	0.018	-4.287	DT	-1.574	-3.546	0.528
9	**Bardarash**	-3.09	0.001	-8.546	DT	-2.390	-8.497	0.528
10	**Mangeshk**	-2.05	0.041	-13.315	DT	-1.468	-13.732	0.371
11	**Bamarne**	2.09	0.034	5.967	IT	1.436	1.968	0.027
12	**Batel**	-1.06	0.289	-2.574	NT	-0.966	-2.910	0.074

Overall, the increasing rate of ETo due to an increase in Tmax and wind speed at some stations, while the decreasing rate of ETo at some other stations may be due to a decrease in wind speed and occurrence of frequent dust storms, which had profound effect on air temperature. In a similar study, Valipour et al., 2021 revealed that the wind speed had the most significant influence on the trend of ETo, particularly in the years with unusual values of ETo.

To further confirm the results of Mann-Kendall trend analysis for annual reference evapotranspiration, two additional tests, namely, Spearman rank correlation and linear regression tests were conducted and the results were displayed in the last columns of Table 3. The sign of the regression line slope, Spearman rank test, and Sen's slope define the direction of the trend of the variable, if sign is positive then it has upward trend and the reverse may be true. It is also apparent from Table 3 that Spearman rank test, linear LR and Sen's slope methods were comparable in estimating the sign of trend. Sen's slope has the advantage over the regression slope in the sense that it is slightly affected data errors and outliers. (Roy and Chakravarty, 2021). Overall, the applied methods offered consistent results. In other words, these tests offered similar performance at the 5% significant level.

It is interesting to note that both MK and SR methods are non-parametric tests and gives poor results when the time series is serially or autocorrelated (Sonali, and Kumar, 2013). Regression analysis as a parametric trend test is more powerful than non-parametric ones, but they require data to be independent and normally distributed. The advantage of Mann-Kendall test lies in the fact that it requires only the data to be independent and can tolerate outliers (Shadmani et al., 2012).

This type of investigation is of primary importance for water resource management in agriculture, climate variability analysis (Roy and Chakravarty, 2021) and the investigation could be extended, where database on this topic is expanded.

3.4. Reference Evapotranspiration Time Series Modeling

3.4.1. Annual Reference Evapotranspiration Time Series Modeling

The best model for forecasting annual reference evapotranspiration time series at each station was identified and the results were displayed in Table 4 .It is obvious from Table 4 that the time series of most of the stations (8 stations out 12 stations) were subjected to non-seasonal first differencing to make the series stationary. Among the best ARIMA models, the form (0,1,0) had the highest frequency followed by (0,1,1). It is noteworthy to mention the data series was initially subjected to plot of autocorrelation function (ACF) and partial autocorrelation. This step was considered as an initial stage for model identification and as a guide to obtain the optimum solution proficiently. Thereafter, many tentative models were examined, at each station. To attain this objective, selected values of p and q, ranging

between 0 and 3 were examined and the corresponding model orders that gave minimum values Nom.BIC, AICc, AIC and BIC were selected. With no exception, all p-values for that Ljung-Box test were more than 0.05. This implies that the proposed models are appropriate for forecasting annual evapotranspiration

To further confirm the adequacy of proposed models, some selected performance indicators such MRSE, MAE and MAPE were also displayed in Table 4. As can be noticed, the mean absolute error varied from a minimum of 3.817 mm at Zawita station to maximum of 129.03 mm at Akre station. Additionally, the results indicated that the mean absolute percentage of error (MAPE) is below 10% indicating that these models can forecast future reference evapotranspiration.

Additionally, ACF and PACF of the residuals were plotted at different lag times to check the adequacy of the proposed models and disclose any misspecification (Anderson, 1976). This was done by testing the ACF and PACF of these residuals at deferent lags. Plotting the results of these plots revealed there was no spike at any lag signifying that the residual process is random. Another attempt was also made to verify the adequacy of the proposed models through checking the normality of the residuals via plotting histograms, Q-Q plots and the scatter plot of type residual. The residuals of the best fit models were checked by plotting normal. Due to space limitations, these plots were not show. However, the residual scatter plot was not characterized by having no pattern. On the other hand the other plots indicated that the residuals have a distribution with slight deviation from normal distribution.

Table (4): The best fit ARIMA models for forecasting the annual ET_0 at 10 stations selected over the study area.

#	Station	Ljung-Box Q(18)		Test of Performance							
		Statistics	Sig.	RMSE	MAPE	MAE	Norm.BIC	AICc	AIC	BIC	ARIMA-model
1	**Duhok**	18.17	0.378	83.21	5.29	69.86	9.14	236.93	236.32	238.22	(1,1,0)
2	**Zakho**	22.44	0.168	42.52	2.72	34.87	7.81	211.84	211.09	212.98	(0,1,1)
3	**Akre**	22.20	0.223	84.37	4.71	67.72	9.03	253.17	252.94	253.88	(0,1,0)
4	**Amedi**	20.17	0.323	84.63	4.53	57.95	9.03	230.13	229.89	230.85	(0,1,0)
5	**Semel**	16.74	0.472	93.63	5.15	68.88	9.38	242.18	241.38	243.16	(0,1,1)
6	**Zawita**	11.94	0.803	81.18	3.99	49.96	9.10	191.75	190.82	192.37	(0,1,1)
7	**Shekhan**	13.42	0.707	63.54	3.07	44.55	8.60	299.09	298.24	299.91	(0,0,1)
8	**Sarsing**	14.52	0.713	62.78	3.58	42.65	8.34	181.71	181.43	182.20	(0,1,0)
9	**Bardarash**	23.89	0.122	63.78	3.58	51.84	8.61	251.82	250.82	252.23	(0,0,1)
10	**Mangeshk**	11.56	0.869	105.26	5.87	72.93	9.46	115.55	113.15	113.31	(0,1,0)
11	**Bamarne**	19.55	0.359	99.20	4.38	59.19	9.36	187.28	186.22	186.50	(0,1,0)
12	**Batel**	11.7	0.18	58.65	3.49	48.93	8.64	181.04	179.97	180.03	(0,0,1)

3.4.2. Monthly Reference Evapotranspiration Time Series Modeling

The same methodology described for forecasting annual reference evapotranspiration was followed to identify the best-fit model for forecasting monthly reference evapotranspiration at the study stations and the results were presented in Table 5. With one exception, the most appropriate model is comprised of SARIMA $(1, 1, 1)(0, 1, 1)_{12}$. It is worth noting that Bayesian Information Criterion (BIC) criterion was applied during model selection to avoid excessive fitting errors (Akaike, 1974). The models with the lowest values for the Bayesian Information Criterion (BIC) were selected.

Prediction-error criteria such as MRSE, MAE and MAPE were also considered to select the final model for forecasting at each stations. It was also noticed that with one exception the mean absolute error was less than 15 mm at the study stations. One the other hand, it was noticed that the mean absolute percentage error (MAPE) did not exceed 14% in 75% of the existing stations.

It seems from the above results that the developed model provides reasonable and adequate estimates, compared to other methods.

These results indicate that the developed SARIMA model provides reasonable and adequate estimates for such studies. This result is on line with the findings of Aghelpour et al.(2021) who reported that the SARIMA is more appropriate for monthly ET0 forecasting under all the climatic condition, on account of its simplicity and parsimony.

It was also obvious from examining the ACF and PACF residuals at deferent lags, the autocorrelation coefficients were not significantly different from zero. This implies that here were no significant values for both ACF and PACF functions for the model residuals. These functions were not displayed during the current study due to space limitations.

Table (5): Selection of the best model for monthly evapotranspiration forecasting at different stations based on AIC and BIC.

#	Station	Ljung-Box Q(18)		Test of Performance				
		Statistics	Sig.	MAPE	RMSE	MAE	Norm.BIC	ARIMA-model
1	**Duhok**	22.657	0.051	9.29	10.483	7.799	4.66	(3,1,1)(0,1,1)
2	**Zakho**	7.030	0.957	11.5	14.493	7.268	5.467	(1,1,1)(0,1,1)
3	**Akre**	14.997	0.452	12.75	17.335	12.466	5.825	(1,1,1)(0,1,1)
4	**Amedi**	17.095	0.313	13.21	14.929	10.622	5.526	(1,1,1)(0,1,1)
5	**Semel**	34.759	0.003	12.41	17.012	11.858	5.793	(1,1,1)(0,1,1)
6	**Zawita**	20.467	0.155	8.39	9.772	7.171	4.696	(1,1,1)(0,1,1)
7	**Shekhan**	2.865	0.99	17.06	101.35	35.680	9.394	(1,1,1)(1,0,1)
8	**Sarsing**	8.869	0.884	9.79	11.281	7.422	4.984	(1,1,1)(0,1,1)
9	**Bardarash**	19.232	0.23	12.09	13.591	10.307	5.372	(1,1,1)(0,1,1)
10	**Mangeshk**	21.231	0.130	26.52	18.97	13.65	6.152	(1,1,1)(0,1,1)
11	**Bamarne**	22.331	0.099	27.55	18.259	13.86	6.01	(1,1,1)(0,1,1)
12	**Batel**	14.997	0.452	9.65	13.306	**9.721**	5.377	(1,1,1)(0,1,1)

Ljung–Box Q test offered an additional confirmation that the estimated residuals of the time series at monthly scale met the demand of a white-noise series. The P-value was ≥ 0.05 at the study stations, suggesting there is no evidence for non-zero autocorrelations at different lags.

Like annual reference evapotranspiration, graphical representation of residuals for monthly reference evapotranspiration in form of histogram, Q-Q-plot and scatter plot revealed that the residuals are normally distributed and free of autocorrelation. It is commendable to mention that such type of study will be of vital importance in the planning and management of water resources.

3.5. Reference Evapotranspiration Forecasting

Based on the optimum SARIMA models, reference evapotranspiration forecasts were obtained for different station sites from January 2023 to December of the year 2025. The forecasting values encompassed forecast during the study period and forecast beyond the sample (study) period (Fig.3). The former was used to develop confidence in the model and the latter was used to simulate forecasts beyond the study period for future planning of water resources within the area under study.

As can be noticed in Fig.3, All forecasted values lied within 95% confidence interval (not displayed on the graphs). Further, the best fit model forecasts produced a reasonable match with observed monthly reference evapotranspiration. Additionally, it can be observed that the pattern of forecasted values resembles the pattern of the original data series to some extent.

Slight deviation from the original data can also be observed over the hottest months of the year. The acceptable accuracy of the models for predicting monthly reference evapotranspiration for a duration of 36 months justifies its future application over the study region thereby aiding to a better planning and management (Swain et al., 2018).

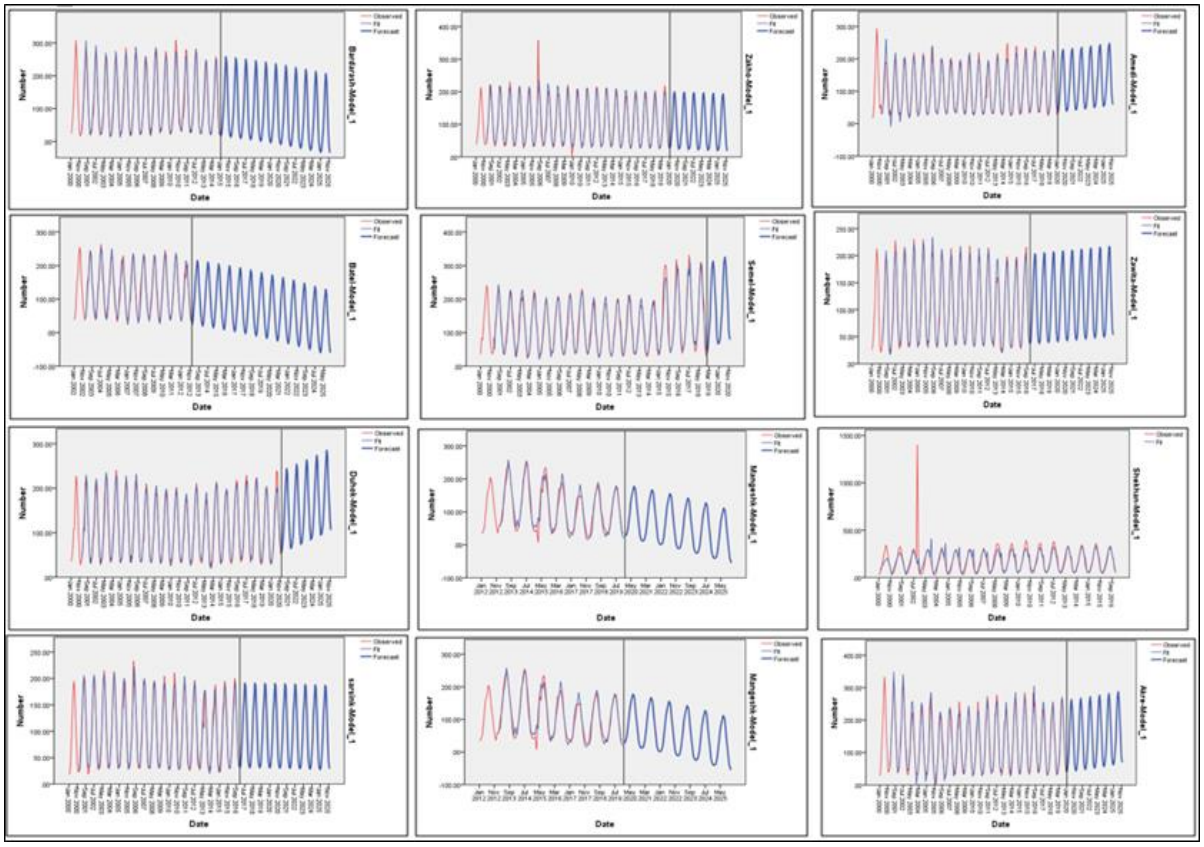

Fig (3): Comparing the observed, fitted and forecasting monthly ET0 at 12 station selected over the study area.

It is interesting to note that the accurate predictions help for adopting better agronomic practices for crops besides crop planning and proper disaster management in risk zones and providing timely relief to those in affected areas.

3.6. Estimation of Reference Evapotranspiration by Different Interpolation Techniques

To study the spatial distribution behavior of reference evapotranspiration over Duhok governorate spatial interpolation was conducted on the average values of annual reference evapotranspiration of 12 stations distributed over the investigated area. The interpolation schemes encompassed IDW, Ordinary Kriging, Universal Kriging and Spline (Table6).

One-way ANOVA test was conducted to show where there are significant differences among different interpolation schemes and the results were displayed in Table. As can be observed in Table the resulting P-value is greater than 0.05. This indicates that the null hypothesis cannot be rejected. In other words, there is evidence that an actual difference did not exist between different methods of interpolation at the indicated level of significance. Calculation of the coefficient of residual mass coefficient (CRM) statistics indicated that UK methods tended slightly to overestimate ETo, while the remaining methods tended to slightly under estimate this agroclimatic parameter. This result is in concordance with finding of Ibrahim and Nasser (2015), who noticed that the IDW method overestimates the climatic variables values, while kriging method underestimated these values.

Table. (6): Average actual and predicted Interpolated ET_0 values for 12 stations.

Stations	Av. Actual ET_0 (mm)	Estimated ET_0 (mm)			
		IDW	Ordinary Kriging	Universal kriging	Spline
Duhok	1335.72	1338.93	1360.89	1392.3	1310.22
Zakho	1297.29	1383.07	1355.75	1407.5	1439.32
Zawita	1415.92	1339.45	1347.03	1399.9	1399.19
Akre	1288.62	1378.98	1379.52	1415.4	1453.32
Mangeshk	1367.42	1348.82	1351.43	1380.2	1328.63
Bamarne	1279.47	1358.17	1359.43	1338.2	1335.49
Amedi	1458.12	1322.11	1351.34	1406.7	1408.22
Semel	1200.51	1375.59	1366.11	1374	1337.02
Batel	1466.58	1292.52	1316.06	1356.1	1169.83
Sarsing	1322.27	1351.95	1361.37	1409.6	1403.06
Bardarash	1400.94	1358.24	1348.39	1430.4	1198.18
Shekhan	1400.40	1360.50	1348.44	1391.7	1454.89

Table 7 presents some selected performance indicators for estimating ETo at annual and monthly scales by different interpolation schemes. In general, the IDW and spline schemes method exhibited highest and lowest accuracy. Judging from these criteria, it can be inferred from the results of the first three methods yielded comparable results. The results also indicated that the mean absolute error percentage (MAEP) of these three methods was below 20% for annual, January, April, July and October reference evapotranspiration time series. However, based on MAE, MAPE, RMSE, D, and NS indicators collectively from cross-validation tests, the order of effectiveness of the interpolation methods will be as follows: IDW > OK> UK> Spline. In a similar study by Hodam et al. (2017), it was observed that IDW outperformed kriging method in almost all the study cases. Therefore, they recommended the former scheme for spatial interpolation of ETo and its leading meteorological parameters. Zhou and Michalak (2009) highlighted that ordinary kriging is not precise because it requires uniform distribution, which can be seldom met. The performance of interpolation schemes is highly reliant on distribution and the spatial density of weather stations in the area under study (Vogt et al., 1997).

Table (7): The performance indicators for estimating ET_0 at different time scales using different interpolation methods.

Data	Criteria/Methods	IDW	OK	UK	Spline
Annual	**MAE**	79.213	75.49	70.15	105.14
	MAPE	5.9	5.6	5.3	7.8
	RMSE	96.46	96.46	93.23	90.58
	D	0.231	0.200	0.420	0.253
	NSE	-0.599	-0.320	-0.272	-0.446
January	**MAE**	5.458	4.79	5.965	8.638
	MAPE	16.2	14.1	17.9	26.9
	RMSE	7.20	20.84	38.47	40.99
	D	0.98	0.98	0.98	0.66
	NSE	-0.59	-0.38	-0.01	-0.29
April	**MAE**	16.36	16.6	17.893	20.342
	MAPE	14.4	14.7	16	17.8
	RMSE	6.56	21.66	37.84	44.50

	D	0.99	0.98	0.98	0.98
	NSE	-0.32	-0.49	-1.91	-0.52
July	**MAE**	27.38	27.6	30.044	41.47
	MAPE	10.9	11.2	12.2	16.7
	RMSE	7.78	23.02	37.80	54.34
	D	0.99	0.99	0.99	0.98
	NSE	-0.86	-0.68	-0.045	-1.26
October	**MAE**	26.97	28.4	38.183	36.18
	MAPE	20.4	21.4	31.9	28.4
	RMSE	14.30	29.26	50.08	55.13
	D	0.96	0.94	0.94	0.97
	NSE	-5.28	-1.72	-0.68	-1.33

To confirm the authenticity of the results of the interpolation methods, distribution of the mean absolute error of different interpolation methods was presented using Box –whisker plots (Fig3). As can be noticed in Fig3. that with one exception, the boxes of the spline method have the longest box and its median line is located slightly above those of the other interpolation methods under most cases. This plot unveils that the spline has the lowest performance and its residuals are characterized by high variability. On the other hand, it can be observed that the remaining methods produced nearly identical boxes, indicating that these methods produced consistent results. It also apparent from Fig that the top whiskers are longer compared to the whiskers at the bottom of the boxes, signifying that the residual distribution is positively skewed. Additionally, it can be the residual distribution of the annual series is more symmetric than those of the monthly series and free of outliers. The monthly time series were characterized by limited number of outliers.

The Technique for Order Preference by Similarity to Ideal Solution (TOPSIS) was also used for ranking the interpolations methods used in this study. The employed criteria were MAE. MAPE, RMSE, agreement index (d) and Nash-Sutcliffe Efficiency coefficient (NSE), while the four alternatives were the four methods of interpolation. The weights of the criteria were determined using entropy method. After determining the comparatively proximity values to the ideal solution, and they were ranked to evaluate the efficiency of the applied interpolation method (Table8). Overall, it can be observed that the IDW is the optimal for interpolating ETo series followed either by OK or UK. The larger the value of proximity to the ideal solution, the better the interpolation method will be (Liu et al., 2021). It obvious from this study that there is no a unique interpolation method for interpolating climatic elements or factors. The accuracy of a given method is affected by a host of factors such topography, climatic characteristics and sample density the performance of an interpolation method depends on the sample density, climatic condition and topography (Hurtado et al., 2021).

Table (8): Ranking the performance of four interpolation methods for determining the reference evapotranspiration ET0 using entropy-weighted TOPSIS in Duhok governorate.

Dataset	**Interpolation method**	d_i^b	d_i^w	$d_i^b + d_i^w$	$\frac{d_i^w}{d_i^b + d_i^w}$	**Ranking**
Annual ET0	IDW	0.61	0.77	1.375	0.557	1
	Ord.kriging	0.95	0.17	1.123	0.150	4
	Uni.Kriging	0.75	0.72	1.474	0.490	2
	Spline	0.66	0.43	1.093	0.398	3
Monthly ET0 during January	IDW	0.09	11.42	11.515	0.992	1
	Ord.kriging	4.19	7.25	11.440	0.634	2
	Uni.Kriging	11.32	0.48	11.808	0.041	4

	Spline	6.77	5.19	11.965	0.434	3
Monthly ET0 during April	IDW	10.50	4.57	15.068	0.303	2
	Ord.kriging	9.55	2.97	12.522	0.237	3
	Uni.Kriging	3.77	10.53	14.296	0.736	1
	Spline	10.25	1.32	11.573	0.114	4
Monthly ET0 during July	IDW	2.92	7.92	10.842	0.731	1
	Ord.kriging	4.56	5.81	10.374	0.560	3
	Uni.Kriging	9.45	1.89	11.335	0.167	4
	Spline	5.30	8.81	14.108	0.624	2
Monthly ET0 during October	IDW	0.00	11.68	11.683	1.000	1
	Ord.kriging	8.90	2.99	11.887	0.252	2
	Uni.Kriging	11.63	0.29	11.919	0.024	4
	Spline	10.10	1.62	11.722	0.138	3

d_i^b = Euclidean distance between the target alternative and the best alternative
d_i^w = Euclidean distance between the target alternative and the worst alternative:

$\frac{d_i^{\mathbf{w}}}{d_i^{\mathbf{b}} + d_i^{\mathbf{w}}}$ =Similarity to the worst alternative

3.7. Spatial Distribution of Reference Evapotranspiration across the Duhok Governorate.

At the end of the study and after exploring the suitable method of interpolation, the mean annual reference evapotranspiration was displayed after generating the IDW data in GIS environment (Fig4.). In general, the spatial distribution of ETo is inhomogeneous. However, the ETo tends to decrease from the southern part to the mountainous area in the north and from the west to the east. As a whole the effect of changing latitude and topography on changing ET_o is not profound compared to their effects on precipitation.

More attention should be paid on water resource planning to some sites such as Bardarash and Shekhan in the south and Semel and Batel in the west part of the study area. Overall, the interpolation methods provided similar spatial distributions of reference evapotranspiration over the region under study.

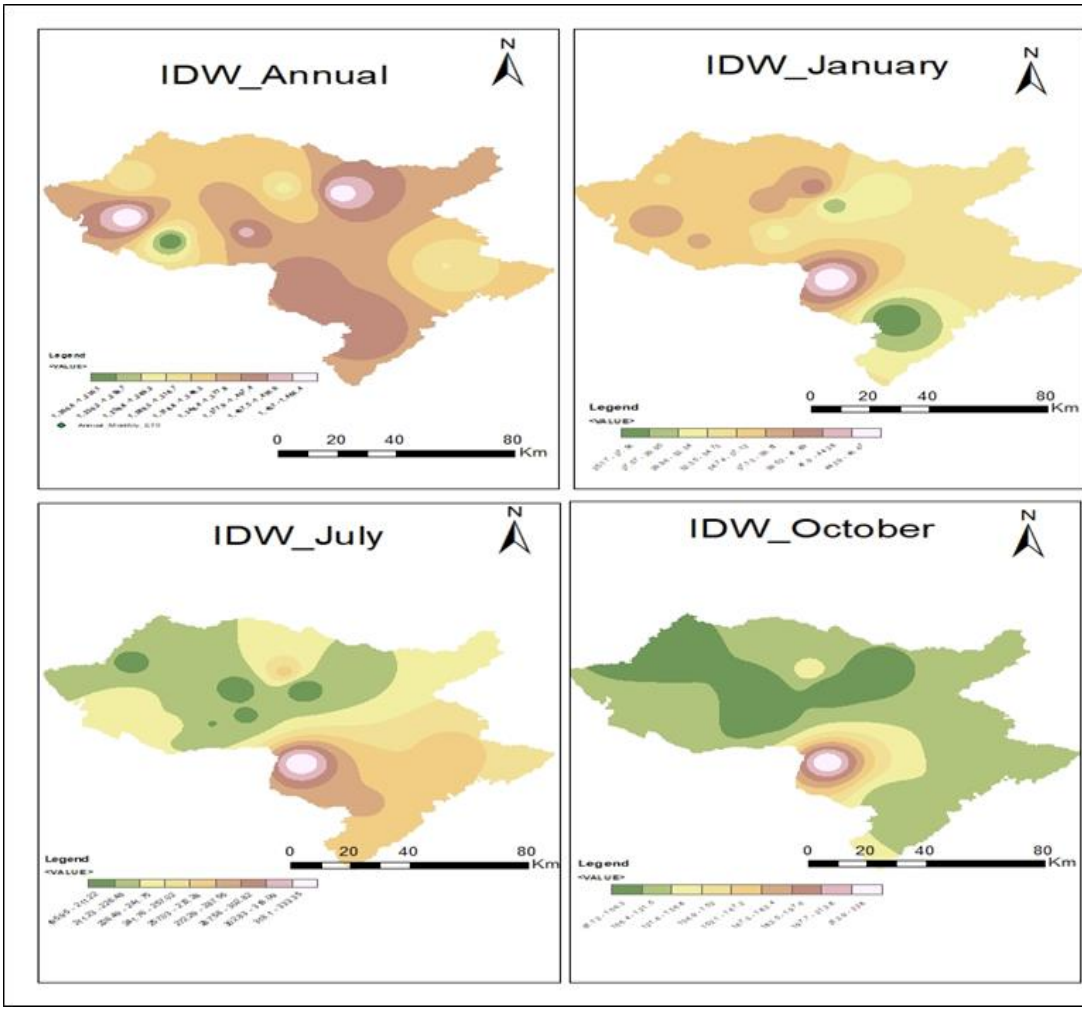

Fig (4): Spatial patterns of the study area based on interpolation methods (IDW) for mean annual and monthly Evapotranspiration.

4. CONCLUSIONS

Overall, the ETo data is characterized by low spatial and temporal variations. Trend analysis elucidated that this agro-climatic factor has a mixture of increasing, decreasing trends and no trend. Parametric and non-parametric trend analysis offered consistent results. Furthermore, it was discerned that the SARIMA model denoted as $(1, 1, 1)(0, 1, 1)_{12}$ can be used for forecasting monthly ET_o time series at more than 90% of the study stations with reasonable accuracy. Additionally it was noticed that IDW had a better performance for estimating ET_o of most of studied time series.

5. REFERENCES

Agha, O. M. A. M., Bağçacı, S. Ç., & Şarlak, N. (2017). Homogeneity analysis of precipitation series in North Iraq. IOSR Journal of Applied Geology and Geophysics, 5(03), 57-63.

Aghelpour, P., Varshavian, V., & Hamedi, Z. (2021). Comparing The Models SARIMA, ANFIS And ANFIS-DE In Forecasting Monthly Evapotranspiration Rates Under Heterogeneous Climatic Conditions.

Akaike, H. (1974). A new look at the statistical model identification. *IEEE transactions on automatic control*, *19*(6), 716-723.

Alhassoun, S., Sendil, U., Al-Othman, A. A., & Negm, A. M. (1997). Stochastic generation of annual and monthly evaporation in Saudi

Arabia. *Canadian water resources journal*, *22*(2), 141-154.

Allen, R. G., Pereira, L. S., Raes, D., & Smith, M. (1998). Crop evapotranspiration-Guidelines for computing crop water requirements-FAO Irrigation and drainage paper 56. *Fao, Rome*, *300*(9), D05109.

Asadi, A., Vahdat, S. F., & Sarraf, A. (2013). The forecasting of potential evapotranspiration using time series analysis in humid and semi humid regions. *American Journal of Engineering Research*, *2*(12), 296-302.

Capozzi, V., Cotroneo, Y., Castagno, P., De Vivo, C., & Budillon, G. (2020). Rescue and quality control of sub-daily meteorological data collected at Montevergine Observatory (Southern Apennines), 1884–1963. *Earth System Science Data Discussions*, *2020*, 1-34.

Shenbin, C., Yunfeng, L., & Thomas, A. (2006). Climatic change on the Tibetan Plateau: potential evapotranspiration trends from 1961–2000. *Climatic change*, *76*(3-4), 291-319.

Chiles, J. P., & Delfiner, P. (2012). *Geostatistics: modeling spatial uncertainty* (Vol. 713). John Wiley & Sons.

Gautam, R., & Sinha, A. K. (2016). Time series analysis of reference crop evapotranspiration for Bokaro District, Jharkhand, India. *Journal of Water and Land Development*, *30*(1), 51.

Gong, L., Xu, C. Y., & Chen, D. L. (2005). Spatial interpolation and analyses of reference evapotranspiration and its temporal trends in Changjiang (Yangtze River) Catchment, China.

Goroshi, S., Pradhan, R., Singh, R. P., Singh, K. K., & Parihar, J. S. (2017). Trend analysis of evapotranspiration over India: Observed from long-term satellite measurements. *Journal of Earth System Science*, *126*, 1-21.

Govay, M. B. I. and Tariq H.K., (2023). Comparative Analysis of Different Techniques for Spatial Interpolation of Rainfall Datasets in Duhok Governorate. The Seybold report. Vol.18, No.01.

Hodam, S., Sarkar, S., Marak, A. G., Bandyopadhyay, A., & Bhadra, A. (2017). Spatial interpolation of reference evapotranspiration in India: Comparison of IDW and Kriging methods. *Journal of the Institution of Engineers (india): Series A*, *98*, 511-524.

Hurtado, S. I., Zaninelli, P. G., Agosta, E. A., & Ricetti, L. (2021). Infilling methods for monthly precipitation records with poor station network density in Subtropical Argentina. *Atmospheric Research*, *254*, 105482.

Mardikis, M. G., Kalivas, D. P., & Kollias, V. J. (2005). Comparison of interpolation methods for the prediction of reference evapotranspiration—an application in Greece. *Water Resources Management*, *19*, 251-278.

Marino, M. A., Tracy, J. C., & Taghavi, S. A. (1993). Forecasting of reference crop evapotranspiration. *Agricultural water management*, *24*(3), 163-187.

Mitas, L., & Mitasova, H. (1999). Spatial interpolation. *Geographical information systems: principles, techniques, management and applications*, *1*(2).

Mohan, S., & Arumugam, N. (1995). Forecasting weekly reference crop evapotranspiration series. *Hydrological sciences journal*, *40*(6), 689-702.

Nalder, I. A., & Wein, R. W. (1998). Spatial interpolation of climatic normals: test of a new method in the Canadian boreal forest. *Agricultural and forest meteorology*, *92*(4), 211-225.

Roy, S., & Chakravarty, N. (2021). Rainfall Analysis by Using Mann-Kendall Trend, Sen's Slope and Variability at Six Stations of Andaman & Nicobar Islands.

Shadmani, M., Marofi, S., & Roknian, M. (2012). Trend analysis in reference evapotranspiration using Mann-Kendall and Spearman's Rho tests in arid regions of Iran. *Water resources management*, *26*, 211-224.

Sonali, P., & Kumar, D. N. (2013). Review of trend detection methods and their application to detect temperature changes in India. *Journal of Hydrology*, *476*, 212-227.

Swain, S., Nandi, S., & Patel, P. (2018). Development of an ARIMA model for monthly rainfall forecasting over Khordha district, Odisha, India. In *Recent findings in intelligent computing techniques* (pp. 325-331). Springer, Singapore.

Tabari, H., Grismer, M. E., & Trajkovic, S. (2013). Comparative analysis of 31 reference evapotranspiration methods under humid conditions. *Irrigation Science*, *31*, 107-117.

Tomas-Burguera, M., Beguería, S., Vicente-Serrano, S., & Maneta, M. (2018). Optimal Interpolation scheme to generate reference crop evapotranspiration. *Journal of Hydrology*, *560*, 202-219.

Valipour, M., Banihabib, M. E., & Behbahani, S. M. R. (2012). Parameters estimate of autoregressive moving average and autoregressive integrated moving average models and compare their ability for inflow forecasting. *J Math Stat*, *8*(3), 330-338.

Valipour, M., Bateni, S. M., & Jun, C. (2021). Global surface temperature: a new insight. *Climate*, *9*(5), 81.

Vogt, J. V., Viau, A. A., & Paquet, F. (1997). Mapping regional air temperature fields using satellite-derived surface skin temperatures. *International Journal of Climatology: A Journal of the Royal Meteorological Society*, *17*(14), 1559-1579.

Wang, W. C., Chau, K. W., Cheng, C. T., & Qiu, L. (2009). A comparison of performance of several artificial intelligence methods for forecasting monthly discharge time series. *Journal of hydrology*, *374*(3-4), 294-306.

Wijngaard, J. B., Klein Tank, A. M. G., & Können, G. P. (2003). Homogeneity of 20th century European daily temperature and precipitation series. *International Journal of Climatology: A Journal of the Royal Meteorological Society*, *23*(6), 679-692.

Xu, C. Y., Gong, L., Jiang, T., Chen, D., & Singh, V. P. (2006). Analysis of spatial distribution and temporal trend of reference evapotranspiration and pan evaporation in Changjiang (Yangtze River) catchment. *Journal of hydrology*, *327*(1-2), 81-93.

Zhang, Q., Wang, B. D., He, B., Peng, Y., & Ren, M. L. (2011). Singular spectrum analysis and ARIMA hybrid model for annual runoff forecasting. *Water resources management*, *25*, 2683-2703.

Zhou, Y., & Michalak, A. M. (2009). Characterizing attribute distributions in water sediments by geostatistical downscaling. *Environmental science & technology*, *43*(24), 9267-9273.

شروڤەکرنا رەوت, مودیلکرن و ئافبەرکرنا وئینتەرپولەیسنێ بێن زنجیرێن دەمی ئاماژە بۆ هەلمە-ئاڤ ل ناوچەێن نیمچە هشك ل پارێزگەها دهوكێ

پوختە

هەلمە-ئاڤ ئاماژە (ETo) ئێكە ژ گرنگترین پێكهاتێن خولا هایدرولوجی. هەلسەنگاندن, پێشبینیكرنا ئینتەرپولەیسنێ جهی ل گەل كاریگەریێن گهورینا كەش و هەوای لسەر ڤی گوراوی هەمی هوكاری پشتیوانی ل بكارئینانا تەكنیكی بڕێڤەبرن بو سەرچاوەێن ئاڤ و ل دەستنیشانكرنا سیراتیجیێن گونجای گونجا. ل ڤێرە ئەڤێ تویژینێ بۆ پێشبینیكرنا ودیاركرنا گورانكاریان و دروستكرنا نەخشا ل روكاری زنجیرێن دەمكی بێن ETo لسەر پیڤەرێن دەمكی بێن دجیاواز دەست پێكر. كومەكا داتایان بۆ ڤێ تویژینێ برتی بوون ل داتایێن كەش و هەوای بێ 12 ەیستگەهێن كەشناسیدناف پارێزگەها دهوكێ بۆ ماوێ دنافبەرا 18 هیتا 20 سالان بون بۆ خەملاندنا هەلمە- ئاڤ لدویف مودیلا پینمان مونتیس.

ئەنجام ئاماژێ ب وێ چەندێ ددەن كو نێزیكی 17% ێ ژ ویستگەهان رەوتی زێدەبوونێ هەیە ل ETo بێ سالانە تیشاددەت, ل دەمەكیدا ل ویستگەهێن دیكە رەوت دابەزینا بەرچاڤ نا یەرچاڤ نیشادا. تاقیكرنا پلا سپیرمان شلوڤەكرنا مودا و پاشەكشا هێلا Sen بنیشانە هوشێوە بەلێ قەباریّ دیاواز هەبوون. مودیلاARIMA كو ب (1، 1، 1)(0، 1، 1)12 دیاركر كو گونجاوترین مودێلە بۆ پێشبینیكرنا زنجیرەیێن هەیڤانەل زیدەتر 90% ێ ژ ویستگەهێن هاتینە دەست نیشانركرن دڤێ ڤەكولینێدا. ئەف مودێلە ب پێبینیكەرا ETo هەیڤانە كریە ب هویربینی یەكت گونجایل 36 مەهێن داهاتی. ئەنجام وێ چەندێ ددەن كۆ شێوازێ IDW وپلوتێن سپلاین بگشتی بەرزترین و كێمتریت وردبینی ل زوربەی حالەتەكاندا نیشادا ددەت. دشێن بێژین كۆ شێوازێ IDW، OK و UK ئەنجامێن بەراورد بدەست ئینانە.

تحليل الاتجاهات والنمذجة واستيفاء السلاسل الزمنية المرجعية لتبخر- نتح في المنطقة شبه الجافة في محافظة دهوك

الخلاصة

يعد التبخر- نتح المرجعي (ETo) أحد أهم مكونات الدورة الهيدرولوجية. إن تقييمها والتنبؤ بها والاستيفاء المكاني إلى جانب تأثيرات تغير المناخ على هذا المتغير كلها عوامل داعمة في تطبيق تقنيات الإدارة على الموارد المائية وفي تحديد استراتيجيات التكيف المناسبة. ومن ثم، بدأت هذه الدراسة للتنبؤ بالتغيرات واكتشافها وإنشاء خرائط سطحية للسلاسل الزمنية لـ ETo على نطاقات زمنية مختلفة. تضمنت مجموعات البيانات لهذا البحث المعلمات المناخية المدخلة من 12 محطة داخل محافظة دهوك لفترة زمنية تتراوح من 18 إلى 20 عامًا لتقدير التبخر- نتح المرجعي وفقًا لصيغة بنمان-مونتيث. أشارت النتائج إلى أن حوالي 17% من المحطات أظهرت اتجاهاً متزايداً في ETo السنوي، في حين أظهرت المحطات المتبقية اتجاهات تناقصية كبيرة وغير هامة. اختبار رتبة سبيرمان قدم تحليل المنحدر والانحدار الخطي Sen منحدرات ذات علامات مماثلة ولكن بأحجام مختلفة. كان نموذج ARIMA الموسمي المشار إليه بـ (1، 1، 1)(0، 1، 1)12 هو النموذج الأكثر ملاءمة للتنبؤ بالسلاسل الزمنية الشهرية لـ ETo في أكثر من 90% من محطات الدراسة. تنبأ النموذج المشار إليه بـ ETo الشهري بدقة معقولة خلال الـ 36 شهرًا القادمة. علاوة على ذلك، أشارت النتائج إلى أن طريقة IDW ومخططات الشريحة أظهرت بشكل عام أعلى وأدنى دقة في معظم الحالات. انطلاقًا من العديد من مؤشرات الأداء، يمكن استنتاج أن طرق IDW وOK وUK قد أسفرت عن نتائج قابلة للمقارنة.